Preliminary analysis of the u235o4brc2 evaluation (Rev.1)

A. Trkov

International Atomic Energy Agency, Vienna, Austria

April 2015

Revision1

A processing error was found that caused Doppler broadening to stop at 2 keV. The source file was patched by shifting the energy of the last zero-cross section point in MT 5 from 2 keV to 2.25 keV. The first non-zero cross section is 25 nanobarns at 2.5 keV, therefore the patch is not expected to have any influence in practical calculations. The ACE file and the results were corrected accordingly.

Introduction

An improved resonance parameter file for ^{235}U was prepared by L. Leal from the Oak Ridge National Laboratory, which was combined with the evaluation of the fast neutron energy region by P. Romain et al. from Bruyeres-le-Chatel. The evaluation is labelled “u235o4brc2”.

Main characteristics of the evaluation

Resonance region

The resolved resonance parameters in the energy range up to 2.25 keV were re-evaluated by L. Leal at the Oak Ridge National Laboratory. For a better comparison of the overall effects the cross sections were reconstructed and averaged in the 28-group ABBN structure. In comparison with ENDF/B-VII.1 the total cross section changed by up to 0.5% (see Figure A). The elastic cross sections were increased by about 3 %, except above 1 keV where the increase amounted to 6 % (see Figure B). The largest decrease of the fission cross section was about 1.9 % between 2 eV and 5 eV, where the cross section has a minimum (see Figure C). The capture cross section was decreased steadily above 100 eV by more than 20 % (see Figure D).

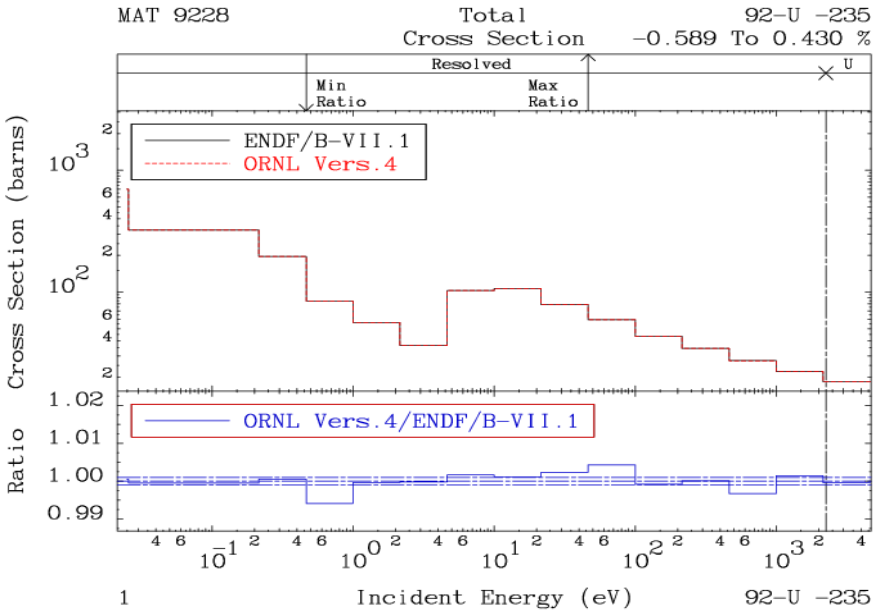

Figure A: Comparison of the total cross section.

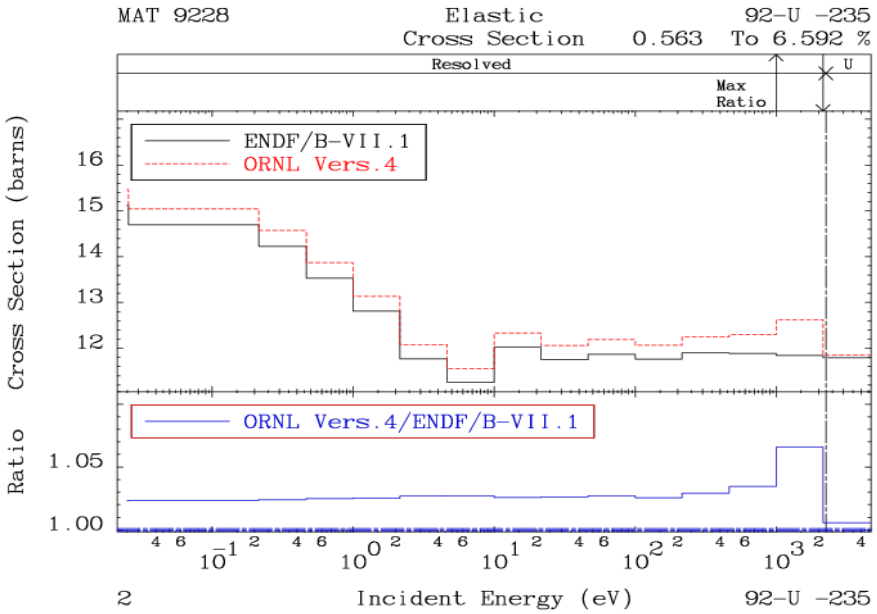

Figure B: Comparison of the elastic cross section.

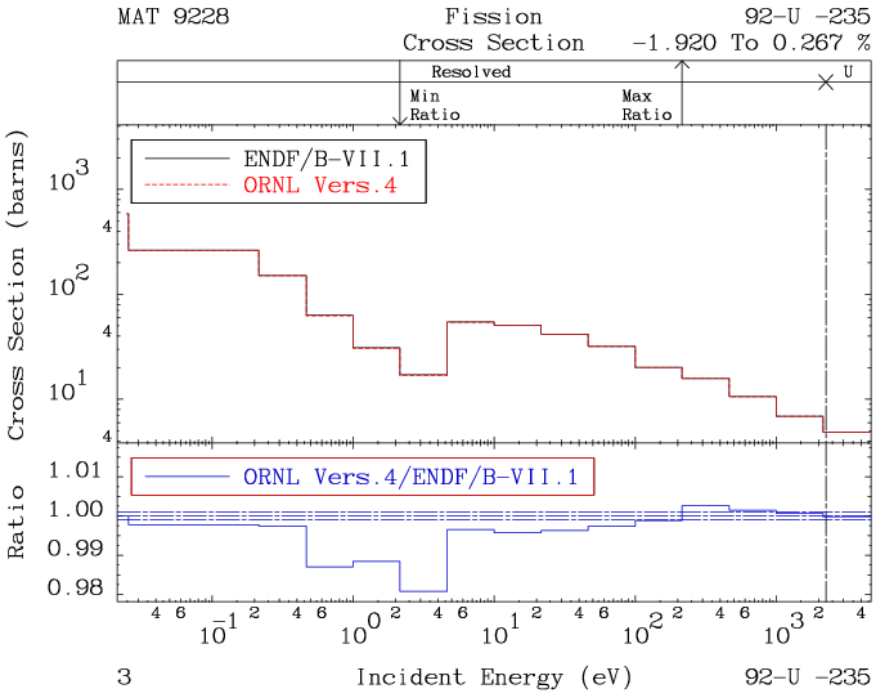

Figure C: Comparison of the fission cross section.

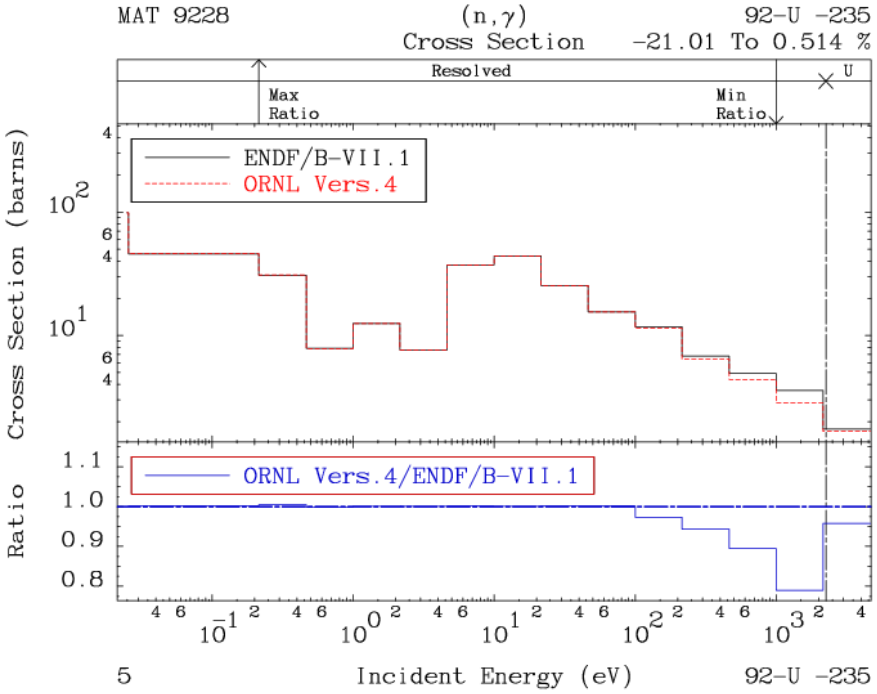

Figure D: Comparison of the radiative capture cross section.

Prompt fission neutron spectrum

The authors adopted the recommendation of N. Kornilov and fitted the average neutron energy of prompt fission neutron spectrum (PFNS) induced by thermal neutrons of 1.97 MeV. This is significantly lower than the current recommendation for the new Standards evaluation using the GMA code and is also much lower than the "u235g6" evaluation with the GANDR code produced at the IAEA, with the average neutron energy of 2.00 MeV. The average energy of the ENDF/B-VII.1 spectrum is 2.03 MeV. The spectra plotted as ratios to a Maxwellian with a temperature of 1.32 MeV are compared in Figure 1.

Cross sections

Taking the ENDF/B-VII.1 evaluation of ^{235}U as reference, several significant differences in the u235o4brc evaluation are observed.

The inelastic cross section is significantly lower. This difference is plausible, considering the latest results obtained with the new optical model potentials, as well as the large uncertainties in the evaluated data and the trends observed in other recent evaluations of the actinides, including the "u238ib44" evaluation for ^{238}U contributed to the CIELO project. A decrease of the inelastic cross section (near its maximum) is known to compensate (partly) the increase in reactivity due to the lowering of the average energy of PFNS in high-leakage highly-enriched uranium solutions (see the Section on benchmarking). The comparison of the inelastic cross sections is shown in Figure 2.

There are differences in other cross sections, but the most outstanding is the large increase in the capture cross sections below 0.1 MeV, which amounts up to nearly 40 % and goes in the opposite direction as the change in the resolved resonance range. Such a large increase needs to be justified, comparing with the latest LANL measurements and the results of the corresponding WPEC Subgroup addressing the capture in ^{235}U. Some of the ICSBEP benchmarks may seem to support a modest increase of the capture, but some others suggest that the current increase is far too big and results in a strong underprediction of reactivity (see the Section on benchmarking).

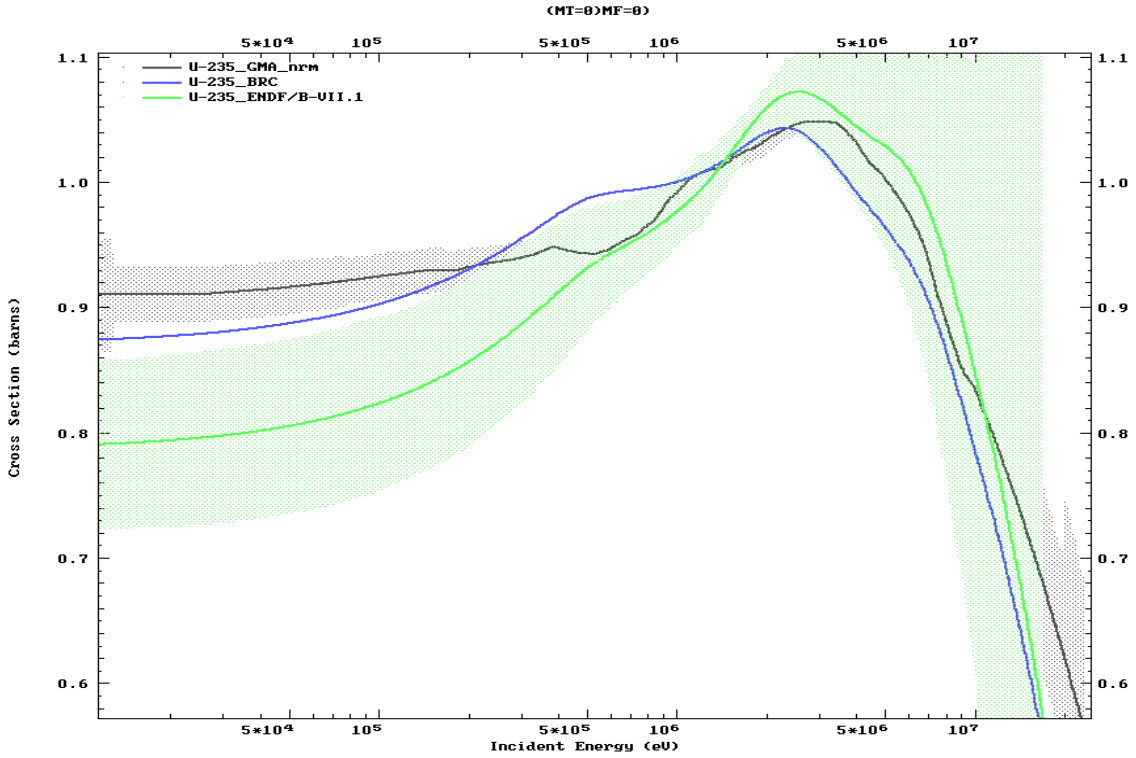

Figure 1: Comparison of thermal-neutron-induced prompt fission spectra plotted as ratios to a Maxwellian at 1.32 MeV.

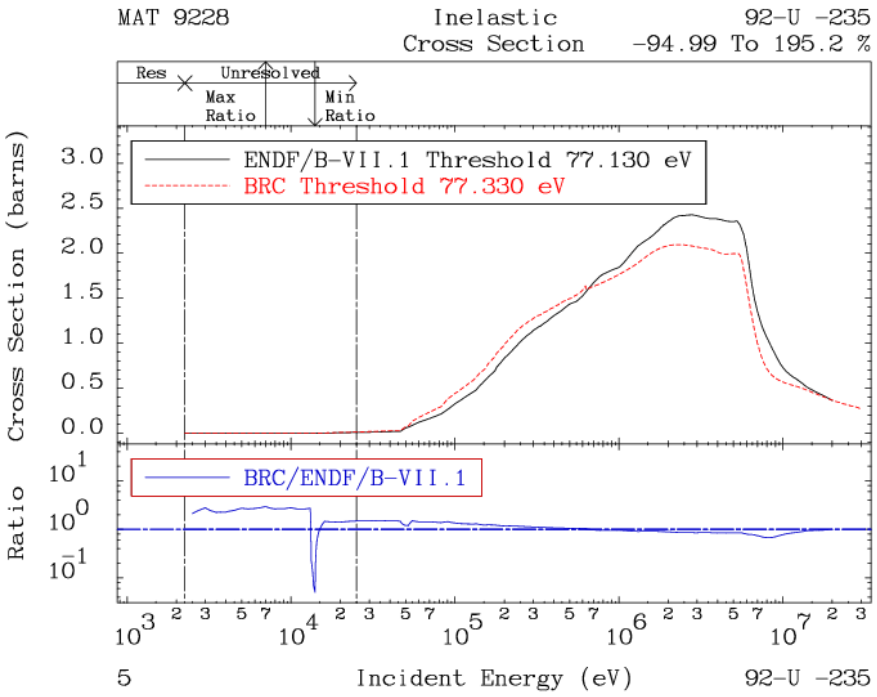

Figure 2: Comparison of the inelastic cross sections in the ENDF/B-VII.1 and BRC evaluations.

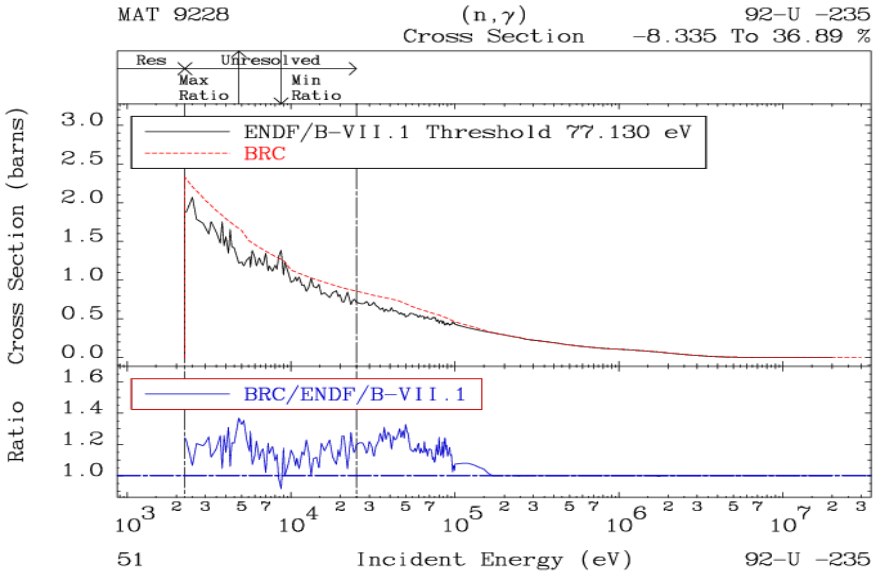

Figure 3: Comparison of the capture cross sections in the ENDF/B-VII.1 and BRC evaluations.

Criticality benchmarks

A broad selection of benchmarks from the ICSBEP collection was analysed.

Table 1: List of ICSBEP benchmarks considered in the analysis.

ICSBEP Name	Short	Common name	Comment
General major benchmarks			
HEU-MET-FAST-001	hmf001	Godiva	
HEU-MET-FAST-028	hmf028	Flattop-25	
IEU-MET-FAST-007	imf007d	Big_Ten(detailed)	
U-238 benchmarks			
HEU-MET-FAST-002	hmf002-1	Topsy-1	
HEU-MET-FAST-002	hmf002-2	Topsy-2	
HEU-MET-FAST-002	hmf002-3	Topsy-3	
HEU-MET-FAST-002	hmf002-4	Topsy-4	
HEU-MET-FAST-002	hmf002-5	Topsy-5	
HEU-MET-FAST-002	hmf002-6	Topsy-6	
IEU-MET-FAST-001	imf001-1	Jemima-1	
IEU-MET-FAST-001	imf001-2	Jemima-2	
IEU-MET-FAST-001	imf001-3	Jemima-3	
IEU-MET-FAST-001	imf001-4	Jemima-4	
MIX-MET-INTER-004	mmi004	ZPR-3/53	
IEU-MET-FAST-002	imf002	Pajarito	
U-238 benchmarks (extended list)			
HEU-COMP-INTER-003	hci003-1	COMET-UH3-1	
HEU-COMP-INTER-003	hci003-4	COMET-UH3-4	

HEU-COMP-INTER-003	hci003-6	COMET-UH3-6
HEU-COMP-INTER-003	hci003-7	COMET-UH3-7
HEU-MET-FAST-008	hmf008	VNIIEF-CTF-bare
HEU-MET-FAST-014	hmf014	VNIIEF-CTF-DU
HEU-MET-FAST-032	hmf032-1	COMET-TU1_3.93in
HEU-MET-FAST-032	hmf032-2	COMET-TU2_3.52in
HEU-MET-FAST-032	hmf032-3	COMET-TU3_1.742in
HEU-MET-FAST-032	hmf032-4	COMET-TU4_0.683in
IEU-MET-FAST-003	imf003-2	VNIIEF-CTF-3
IEU-MET-FAST-004	imf004-2	VNIIEF-CTF-4
IEU-MET-FAST-005	imf005	VNIIEF-CTF-5
IEU-MET-FAST-005	imf005-s	VNIIEF-CTF-5s
IEU-MET-FAST-006	imf006	VNIIEF-CTF-6
IEU-MET-FAST-006	imf006-s	VNIIEF-CTF-6s
IEU-MET-FAST-010	imf010	ZPR-6/9(U9)
LEU-COMP-THERM-008	lct008-01	BW-XI-1
LEU-COMP-THERM-008	lct008-02	BW-XI-2
LEU-COMP-THERM-008	lct008-05	BW-XI-5
LEU-COMP-THERM-008	lct008-07	BW-XI-7
LEU-COMP-THERM-008	lct008-08	BW-XI-8
LEU-COMP-THERM-008	lct008-11	BW-XI-11
LEU-SOL-THERM-002	lst002-1	ORNL-UO2F2
LEU-SOL-THERM-002	lst002-2	ORNL-UO2F2
LEU-SOL-THERM-007	lst007-14	STACY-14
LEU-SOL-THERM-007	lst007-30	STACY-30
LEU-SOL-THERM-007	lst007-32	STACY-32
LEU-SOL-THERM-007	lst007-36	STACY-36
LEU-SOL-THERM-007	lst007-49	STACY-49
HEU thermal solution benchmarks		
HEU-SOL-THERM-009	hst009-1	ORNL_S1
HEU-SOL-THERM-009	hst009-2	ORNL_S2
HEU-SOL-THERM-009	hst009-3	ORNL_S3
HEU-SOL-THERM-009	hst009-4	ORNL_S4
HEU-SOL-THERM-013	hst013-1	ORNL_T1
HEU-SOL-THERM-013	hst013-2	ORNL_T2
HEU-SOL-THERM-013	hst013-3	ORNL_T3
HEU-SOL-THERM-013	hst013-4	ORNL_T4
HEU-SOL-THERM-032	hst032	ORNL_T5
HEU-SOL-THERM-001	hst001-01	R01
HEU-SOL-THERM-001	hst001-02	R02
HEU-SOL-THERM-001	hst001-03	R03
HEU-SOL-THERM-001	hst001-04	R04
HEU-SOL-THERM-001	hst001-05	R05
HEU-SOL-THERM-001	hst001-06	R06
HEU-SOL-THERM-001	hst001-07	R07
HEU-SOL-THERM-001	hst001-08	R08
HEU-SOL-THERM-001	hst001-09	R09
HEU-SOL-THERM-001	hst001-10	R10

HEU-SOL-THERM-042	hst042-1	ORNL_C1	
HEU-SOL-THERM-042	hst042-2	ORNL_C2	
HEU-SOL-THERM-042	hst042-3	ORNL_C3	
HEU-SOL-THERM-042	hst042-4	ORNL_C4	
HEU-SOL-THERM-042	hst042-5	ORNL_C5	
HEU-SOL-THERM-042	hst042-6	ORNL_C6	
HEU-SOL-THERM-042	hst042-7	ORNL_C7	
HEU-SOL-THERM-042	hst042-8	ORNL_C8	
Thorium benchmarks			
HEU-MET-FAST-085	hmf085-5	Comet-Th_2in	
HEU-COMP-THERM-015	hct015-11	SB-1	
HEU-COMP-THERM-015	hct015-15	SB-5	
IEU-COMP-FAST-002	icf002	KBR-18	
IEU-COMP-INTER-001	ici001-19	KBR-19	
IEU-COMP-INTER-001	ici001-20	KBR-20	
IEU-COMP-THERM-005	ict005	KBR-21	Outlier?
HEU-MET-FAST-068	hmf068	KBR-22	
HEU-MET-INTER-008	hmi008	KBR-23	
HEU-COMP-THERM-021	hct021-01	TUPE-001	
HEU-COMP-THERM-021	hct021-02	TUPE-002	
HEU-COMP-THERM-021	hct021-03	TUPE-003	
HEU-COMP-THERM-021	hct021-04	TUPE-004	
HEU-COMP-THERM-021	hct021-05	TUPE-005	
HEU-COMP-THERM-021	hct021-06	TUPE-006	
HEU-COMP-THERM-021	hct021-07	TUPE-007	
HEU-COMP-THERM-021	hct021-08	TUPE-008	
HEU-COMP-THERM-021	hct021-09	TUPE-009	
HEU-COMP-THERM-021	hct021-10	TUPE-010	
HEU-COMP-THERM-021	hct021-11	TUPE-011	
HEU-COMP-THERM-021	hct021-12	TUPE-012	
HEU-COMP-THERM-021	hct021-13	TUPE-013	
HEU-COMP-THERM-021	hct021-14	TUPE-014	
HEU-COMP-THERM-021	hct021-44	TUPE-044	
Tungsten benchmarks			
IEU-MET-FAST-013	imf013	ZPR-9/1	
IEU-MET-FAST-014	imf014-2	ZPR-9/2	
IEU-MET-FAST-014	imf014-3	ZPR-9/3	
HEU-MET-FAST-060	hmf060-4	ZPR-9/4	
HEU-MET-FAST-067	hmf067-5	ZPR-9/5	
HEU-MET-FAST-067	hmf067-6	ZPR-9/6	
HEU-MET-FAST-070	hmf070-7	ZPR-9/7	
HEU-MET-FAST-070	hmf070-8	ZPR-9/8	
HEU-MET-FAST-070	hmf070-9	ZPR-9/9	
HEU-MET-FAST-049	hmf049-1	KFBN2-1cm	
HEU-MET-FAST-049	hmf049-2	KFBN2-3cm	
HEU-MET-FAST-049	hmf049-3	KFBN2-8cm	
HEU-MET-FAST-050	hmf050	KFBN2-f1	
HEU-MET-FAST-052	hmf052	KFBN2-f2	

HEU-MET-MIXED-017	hmm017	KFBN2-f3	
HEU-MET-FAST-084	hmf084-14	Comet-W_1.0in	
HEU-MET-FAST-084	hmf084-25	Comet-W_0.5in	
HEU-MET-FAST-085	hmf085-6	Comet-W_2.0in	
HEU-MET-FAST-003	hmf003-01	Topsy-U_2.0in	Tungsten reflector
HEU-MET-FAST-003	hmf003-02	Topsy-U_3.0in	Tungsten reflector
HEU-MET-FAST-003	hmf003-03	Topsy-U_4.0in	Tungsten reflector
HEU-MET-FAST-003	hmf003-04	Topsy-U_5.0in	Tungsten reflector
HEU-MET-FAST-003	hmf003-05	Topsy-U_6.0in	Tungsten reflector
HEU-MET-FAST-003	hmf003-06	Topsy-U_8.0in	Tungsten reflector
HEU-MET-FAST-003	hmf003-07	Topsy-U_11.in	Tungsten reflector
Zirconium benchmarks			
HEU-MET-FAST-061	hmf061	ZPPR-21F	
HEU-COMP-INTER-005	hci005-16	KBR-16	Outlier?
HEU-COMP-THERM-007	hct007-1	RRCt-1	
HEU-COMP-THERM-007	hct007-2	RRCt-2	Problem with input ?
HEU-COMP-MIXED-003	hcm003-1	RRCm-1	
IEU-COMP-THERM-003	ict003-1	TRIGA C_132	
IEU-COMP-THERM-003	ict003-2	TRIGA C_132	
IEU-COMP-THERM-009	ict009-1	PBF-1	
IEU-COMP-THERM-009	ict009-2	PBF-2	
MIX-MET-FAST-011	mmf011-b	ZPPR-21B	
MIX-MET-FAST-011	mmf011-c	ZPPR-21C	
MIX-MET-FAST-011	mmf011-d	ZPPR-21D	
MIX-MET-FAST-011	mmf011-e	ZPPR-21E	
LEU-COMP-THERM-009	lct009-26	LCT9-26	
LEU-COMP-THERM-009	lct009-27	LCT9-27	
Iron benchmarks			
HEU-MET-FAST-013	hmf013	VNIITF-CTF-SS-13	
HEU-MET-FAST-021	hmf021	VNIITF-CTF-SS-21	
HEU-MET-FAST-024	hmf024	VNIITF-CTF-SS-24	
HEU-MET-FAST-087	hmf087	VNIITF-CTF-Fe	
HEU-MET-FAST-088	hmf088-1	hmf088-1	
HEU-MET-FAST-088	hmf088-2	hmf088-2	
HEU-MET-INTER-001	hmi001	ZPR-9/34	
MIX-COMP-FAST-001	mcf001	ZPR-6/7	
MIX-COMP-FAST-005	mcf005-s	ZPR-9/31	
MIX-COMP-FAST-006	mcf006-s	ZPPR-2	
MIX-COMP-THERM-001	mct001-1	mct001-1	
LEU-COMP-THERM-042	lct042-1	lct042-1	
LEU-COMP-THERM-042	lct042-2	lct042-2	
LEU-COMP-THERM-042	lct042-3	lct042-3	
LEU-COMP-THERM-042	lct042-4	lct042-4	
LEU-COMP-THERM-042	lct042-5	lct042-5	
LEU-COMP-THERM-042	lct042-6	lct042-6	
LEU-COMP-THERM-042	lct042-7	lct042-7	
LEU-COMP-THERM-043	lct043-2	IPEN/MB-01	
LEU-MET-THERM-015	lmt015	lmt015	

LEU-COMP-THERM-087	lct087	lct087
HEU-MET-THERM-013	hmt013-2	hmt013-2
HEU-MET-THERM-015	hmt015	hmt015
HEU-MET-FAST-072	mf072-1	ZEUS_Fe/Cu-1
HEU-MET-FAST-072	mf072-2	ZEUS_Fe/Cu-2
HEU-MET-FAST-072	mf072-3	ZEUS_Fe/Cu-3

The results are presented for several groups of benchmarks separately in Figures 4 – 24, where comparison is made of the results using the pure ENDF/B-VII.1 data (labelled "e71"), the ^{235}U data with the PFNS replaced by the non-model Standards evaluation with the GMA code (labelled "u235g6a", the ^{235}U data with PFNS taken from the "u235o4brc2" evaluation (labelled "u235spbr2"), the ^{235}U data with resonance parameters replaced by the new set from Oak Ridge (labelled "u235o4")and the pure "u235o4br2" evaluation.

The general trend is that a lower average energy of PFNS reduces the reactivity of the fast systems (see Figure 3, for example), but greatly increases the reactivity of the high-leakage highly-enriched uranium solutions (compare "e71" with "u235g6a" and "u235spbrc2" in Figure 5).

The changes to the elastic and capture cross sections in the resonance range only affect certain benchmarks, namely COMET-UH3, KBR-23, FKBN2-f2 and ZPR-9/34. Some benchmarks show a slight decrease in reactivity, but this is far less significant. Generally, the changes in the resonance parameters alone do not improve the agreement with benchmark values. The results are shown in Figures 11 – 17.

The lower inelastic cross section in the "u235o4brc2" evaluation partly compensates the increase in reactivity due to the lower average energy of the PFNS, but the reduction is not sufficient. On the other hand, a similar reduction of the inelastic cross section in the "u235g6a" evaluation would most likely compensate the increase in reactivity almost entirely. The results are shown in Figures 18 – 24, where the effects of the resonance data, the PFNS and the combined offect of the "u235o4brc2" are shown.

A number of benchmarks show a large drop in reactivity when the "u235o4brc2" evaluation is used. See for example Big Ten and Pajarito in Figure 18. The most likely cause of the decrease is the large increase in the capture cross section below 0.1 MeV. Some benchmarks like the ZPR-9 cases in Figure 22, which generally overpredict the reactivity, show large sensitivity to the cross sections in "u235o4brc2", but the swing in the negative direction is far too big.

Conclusions

It is premature to draw definite conclusions; nevertheless, the benchmarking evidence suggests that the average energy of thermal-neutron induced PFNS is indeed lower than that in ENDF/B-VII.1, but probably not as low as in the "u235o4brc2" evaluation. The large increase in the capture cross section in the "u235o4brc2" evaluation requires careful checking. There are strong compensating effects, so utmost care is needed to avoid being lured to wrong adjustment in the evaluations of individual reactions.

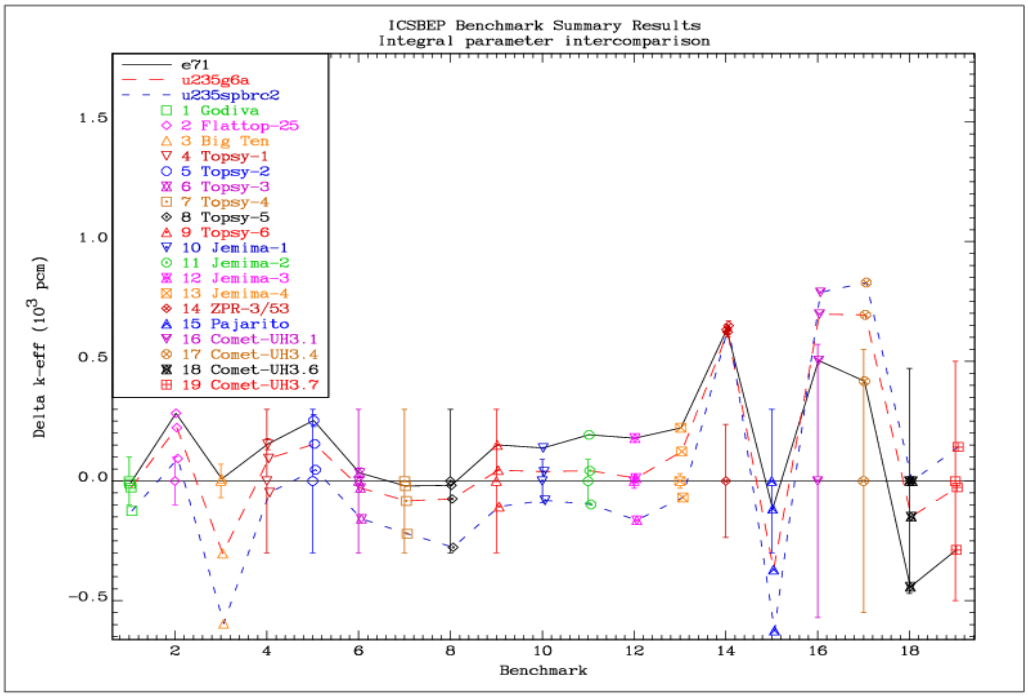

Figure 4: Results for the general major benchmarks.

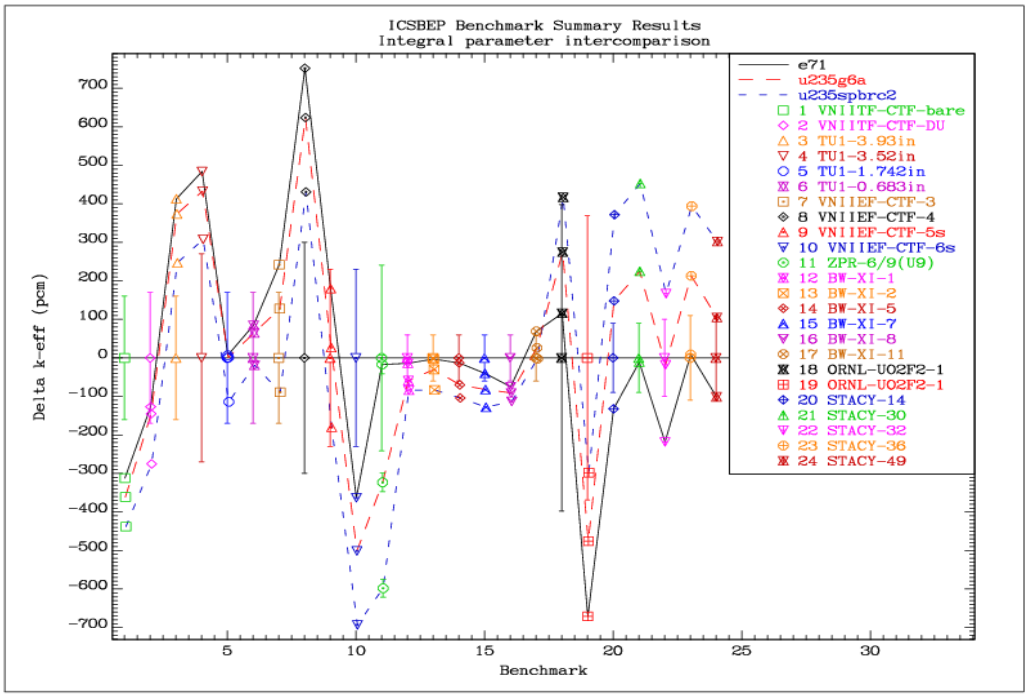

Figure 5: Results for an extended list of general benchmarks.

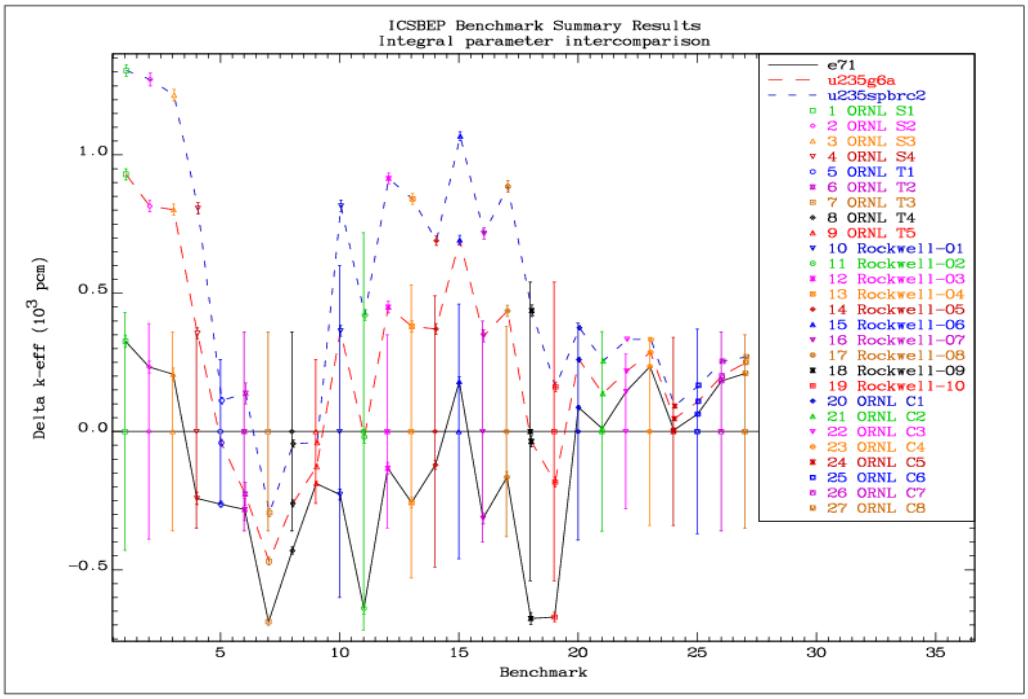

Figure 6: Results for highly-enriched thermal solutions.

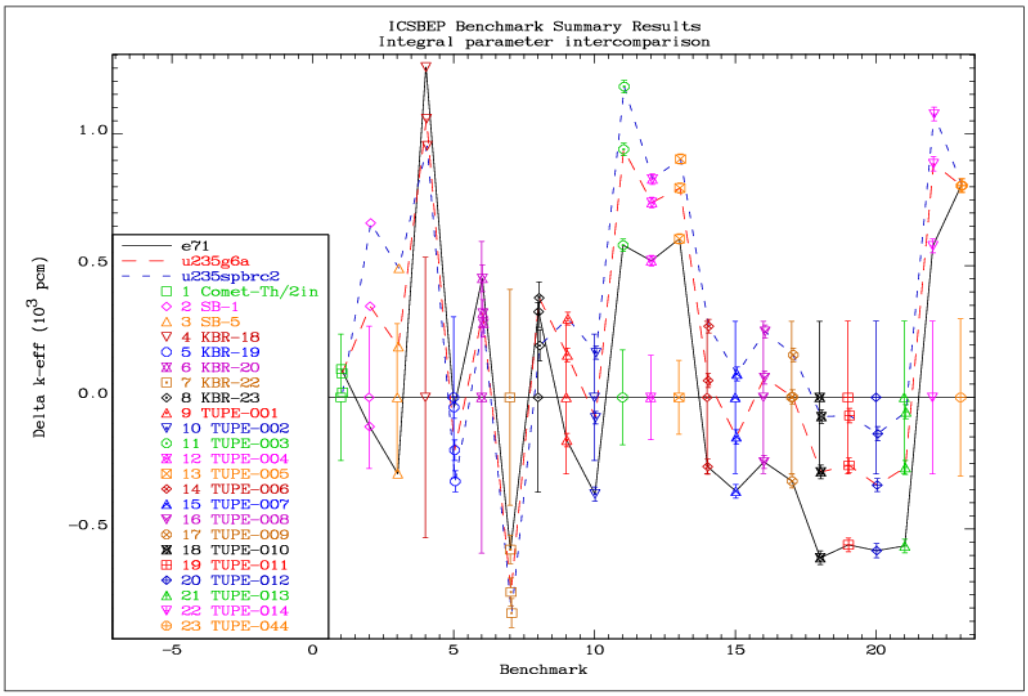

Figure 7: Results for thorium benchmarks.

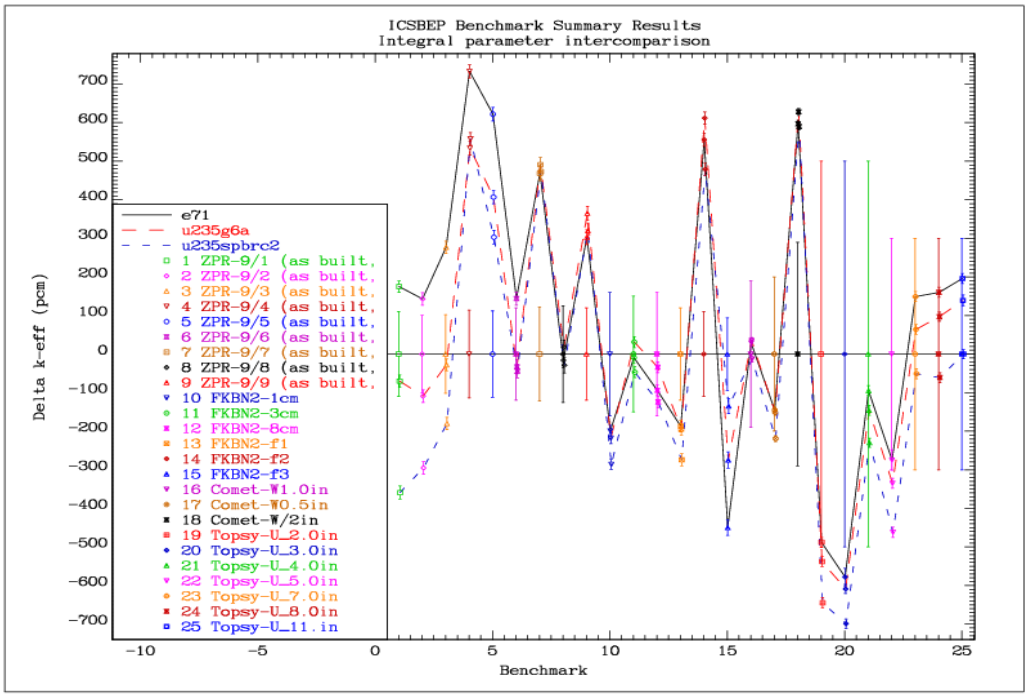

Figure 8: Results for tungsten benchmarks.

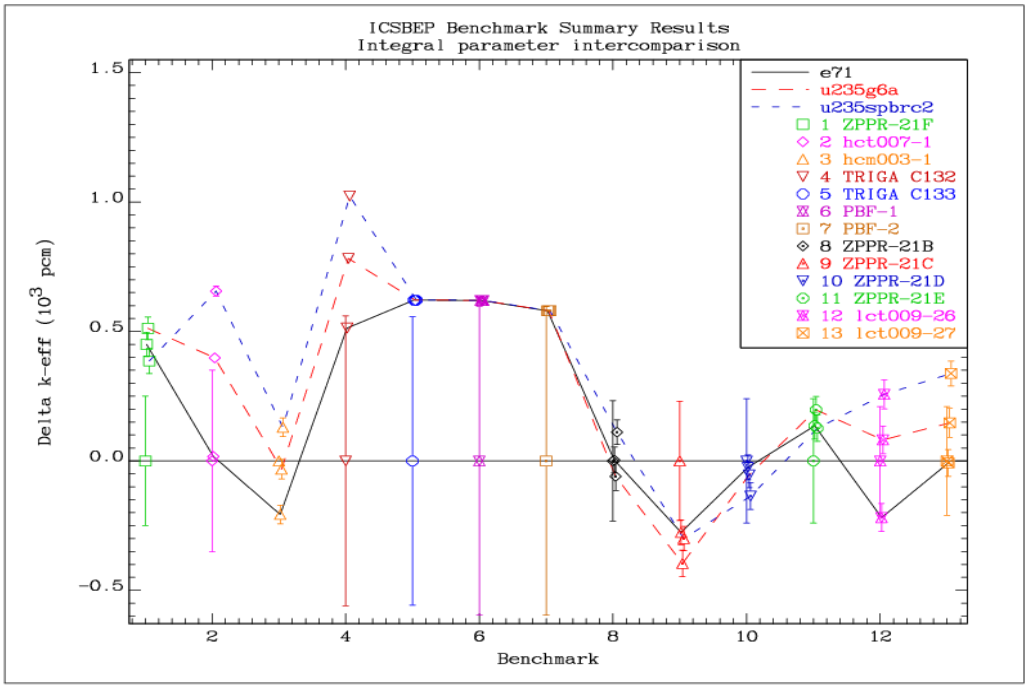

Figure 9: Results for zirconium benchmarks.

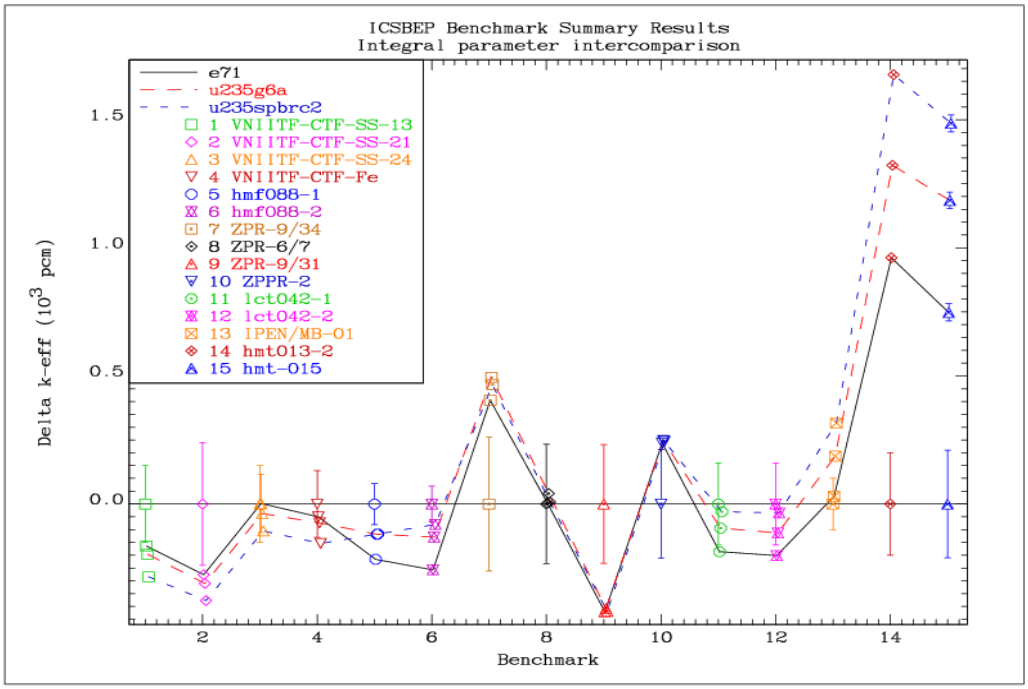

Figure 10: Results for iron benchmarks.

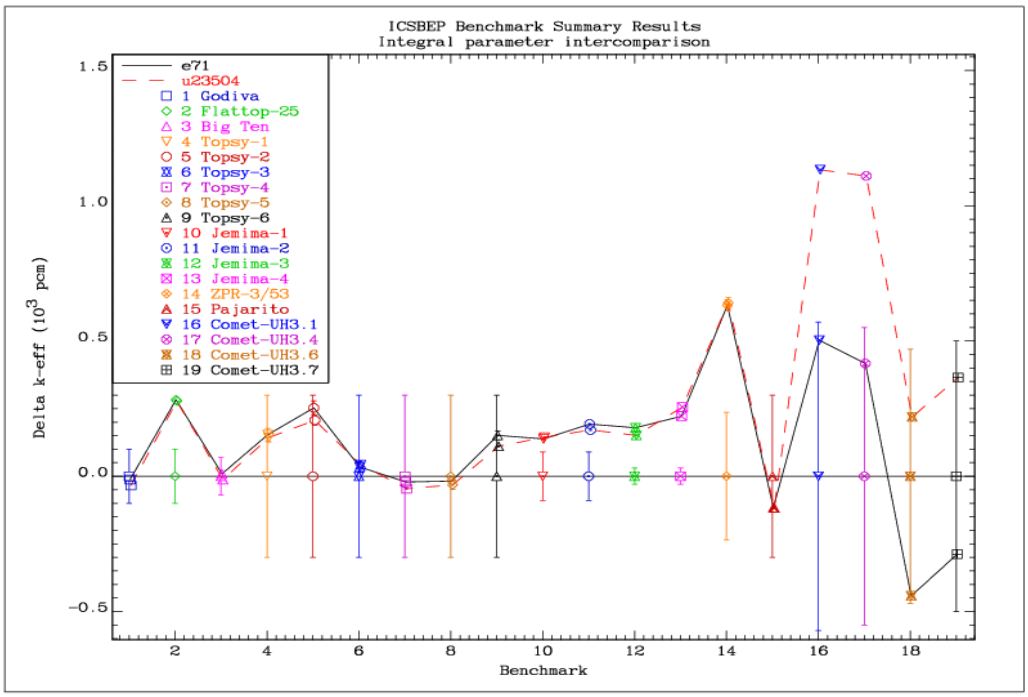

Figure 11: Results for the general major benchmarks.

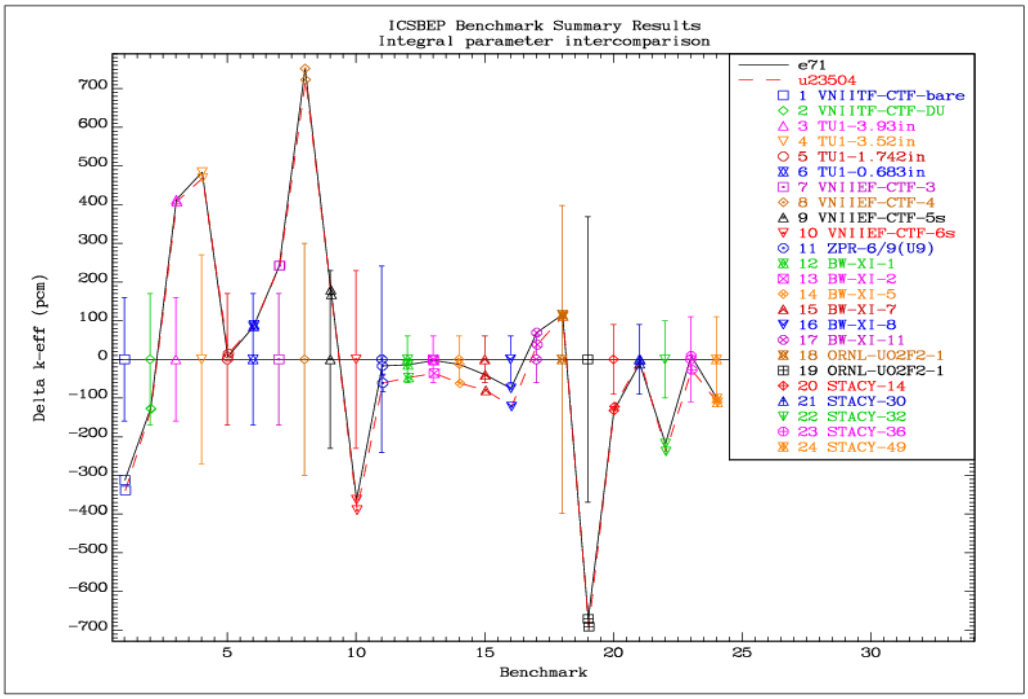

Figure 12: Results for an extended list of general benchmarks.

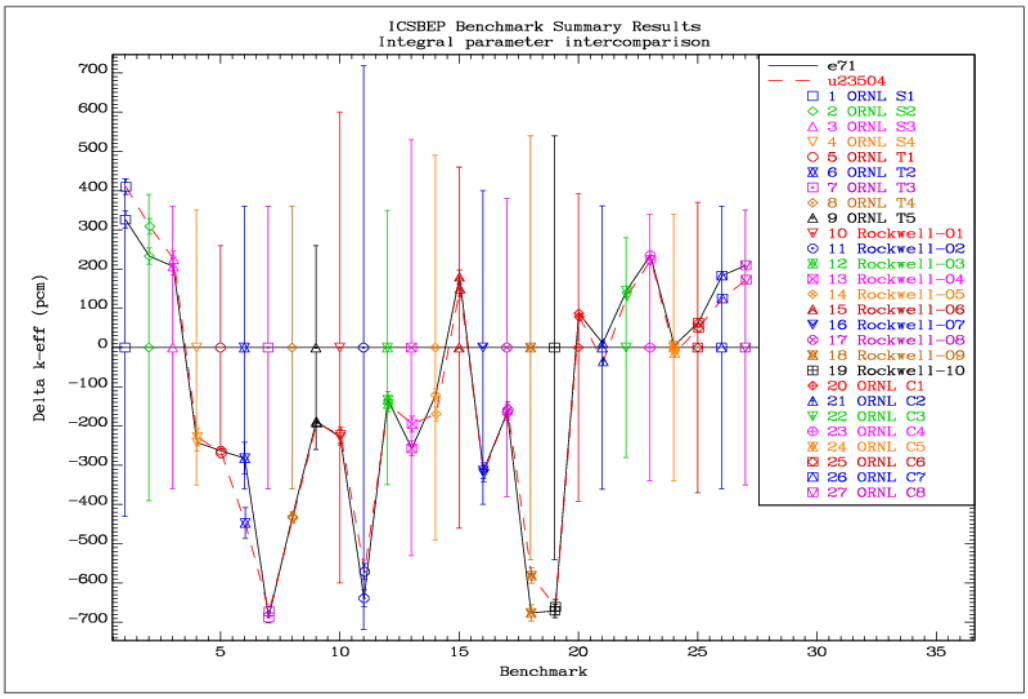

Figure 13: Results for highly-enriched thermal solutions.

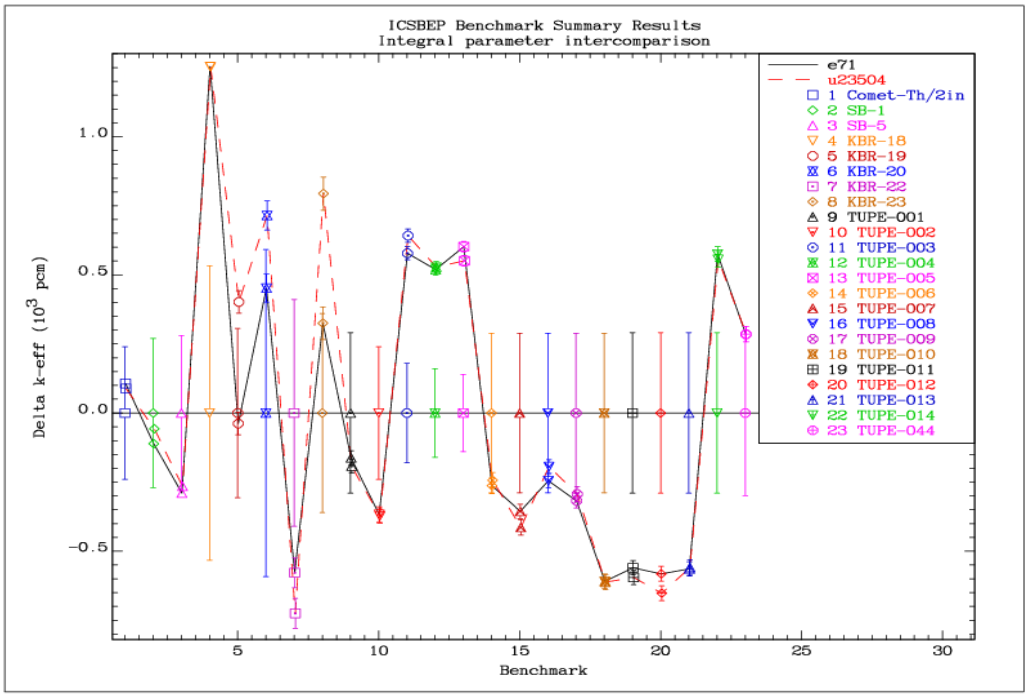

Figure 14: Results for thorium benchmarks.

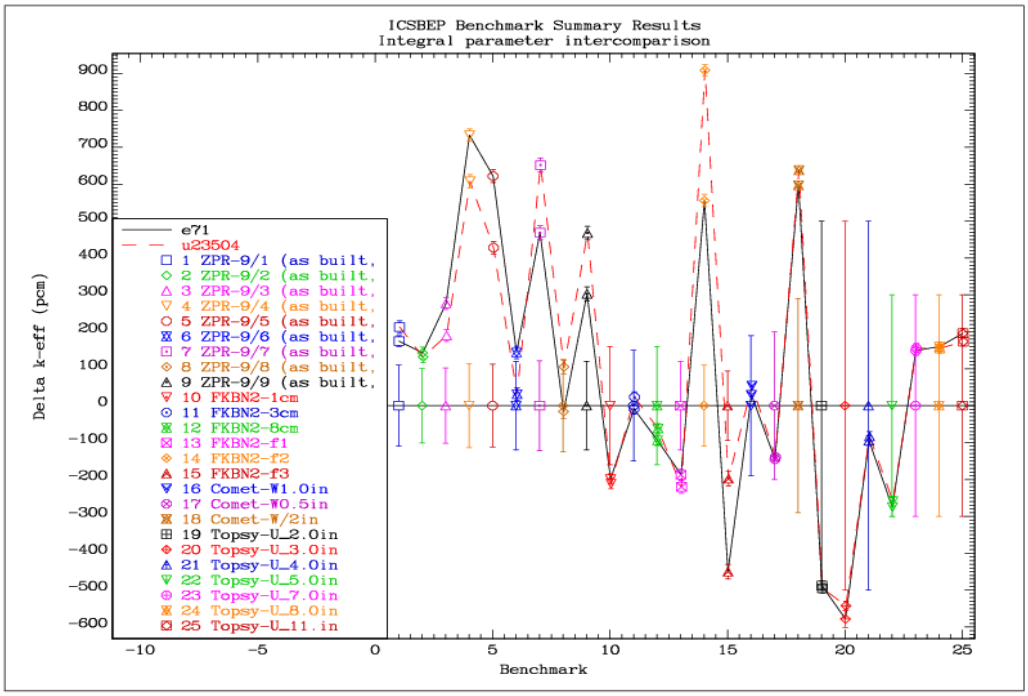

Figure 15: Results for tungsten benchmarks.

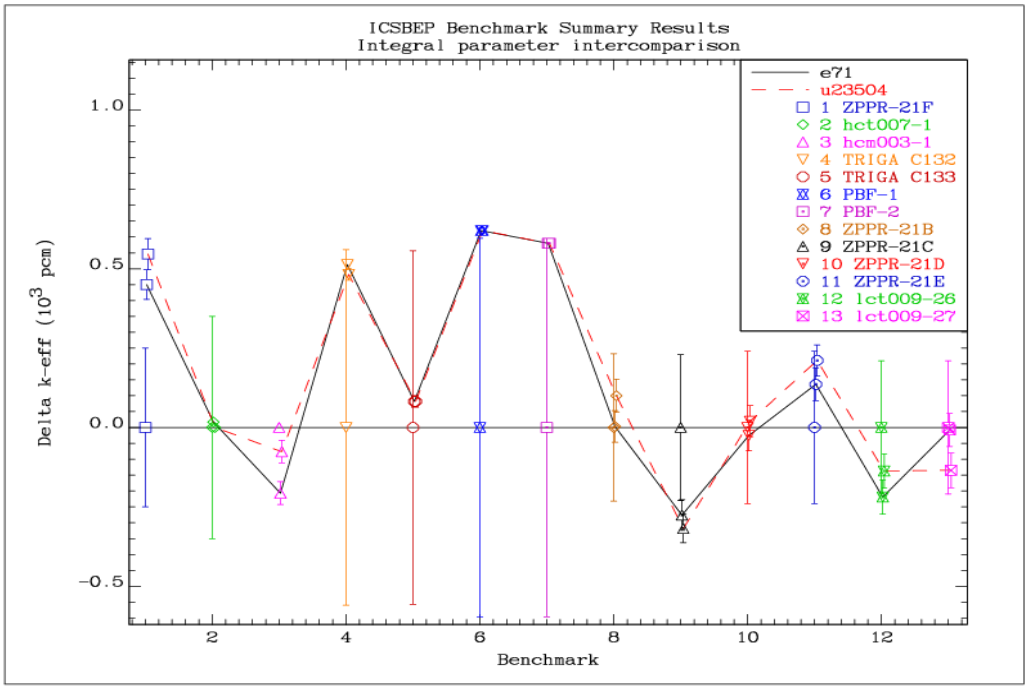

Figure 16: Results for zirconium benchmarks.

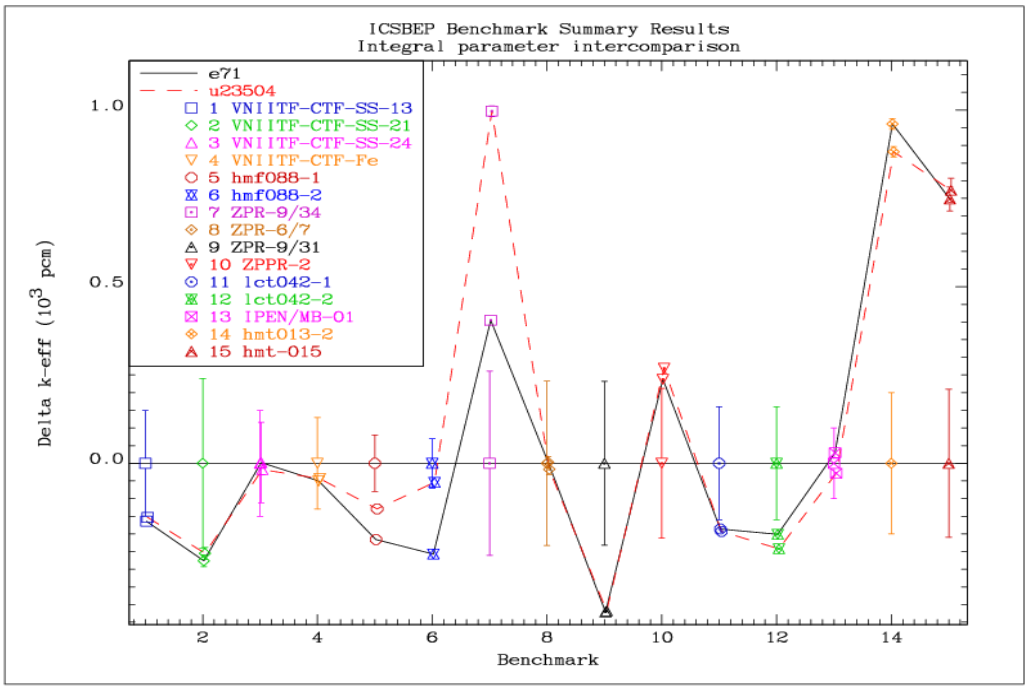

Figure 17: Results for iron benchmarks.

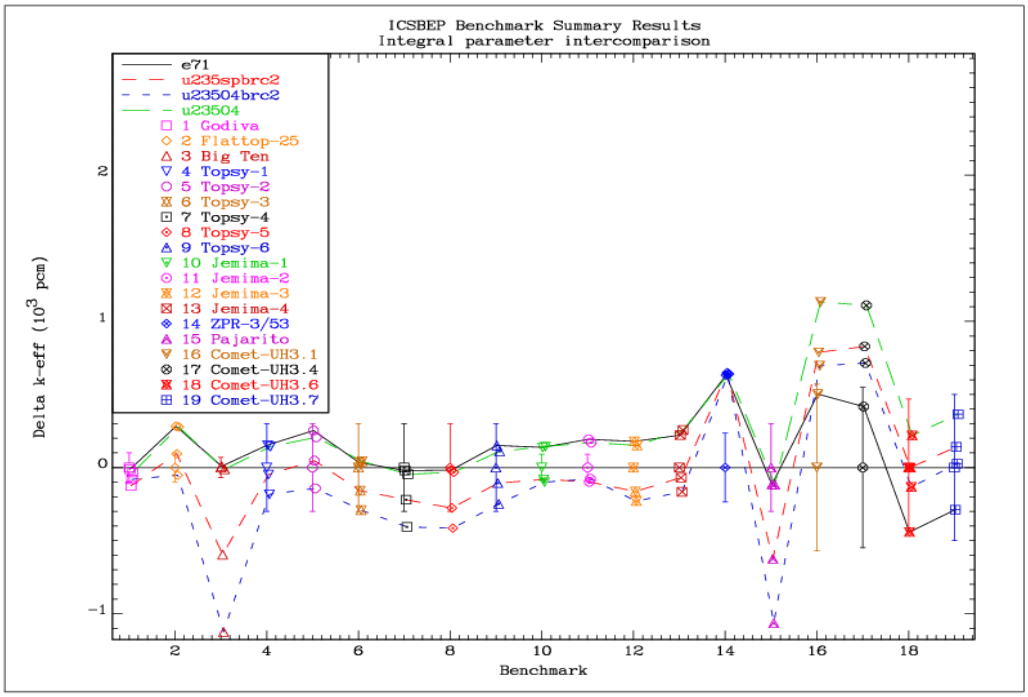

Figure 18: Results for the general major benchmarks.

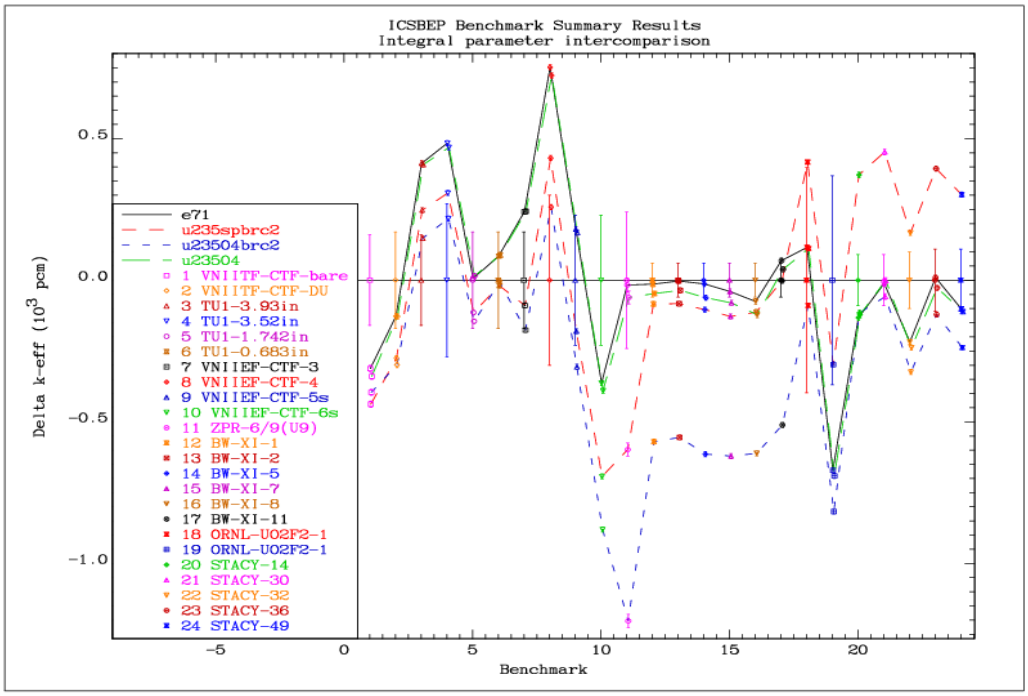

Figure 19: Results for an extended list of general benchmarks.

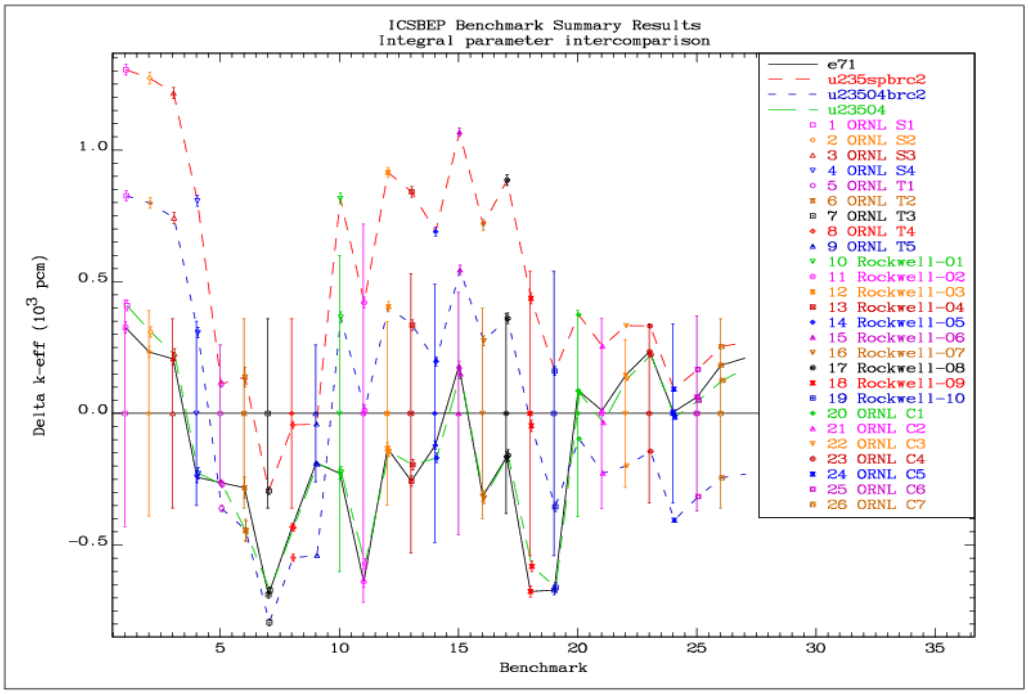

Figure 20: Results for highly-enriched thermal solutions.

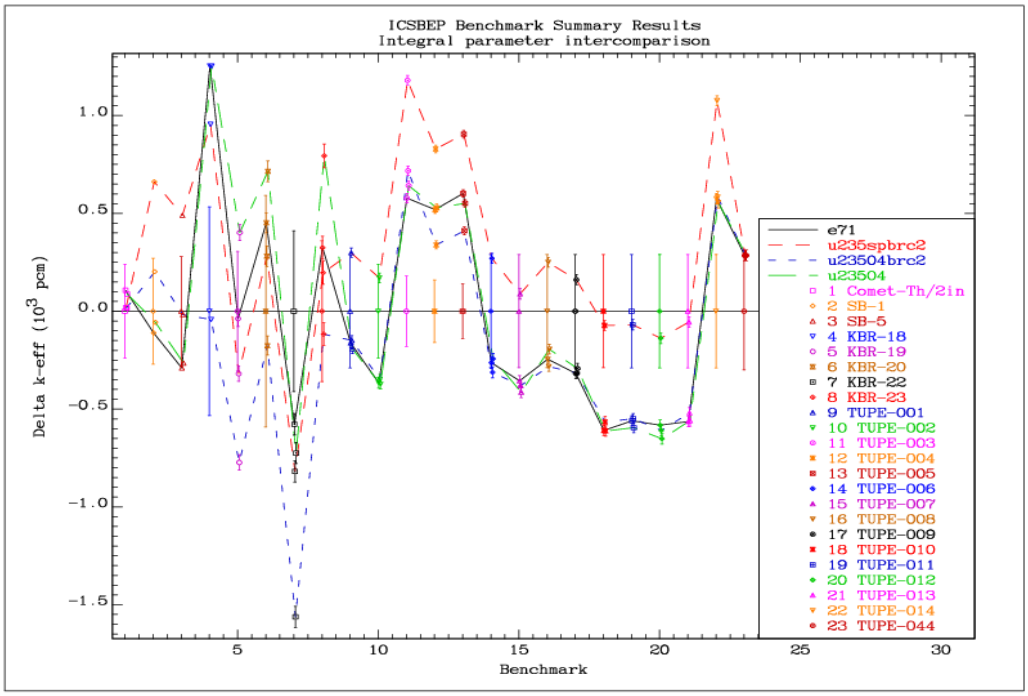

Figure 21: Results for thorium benchmarks.

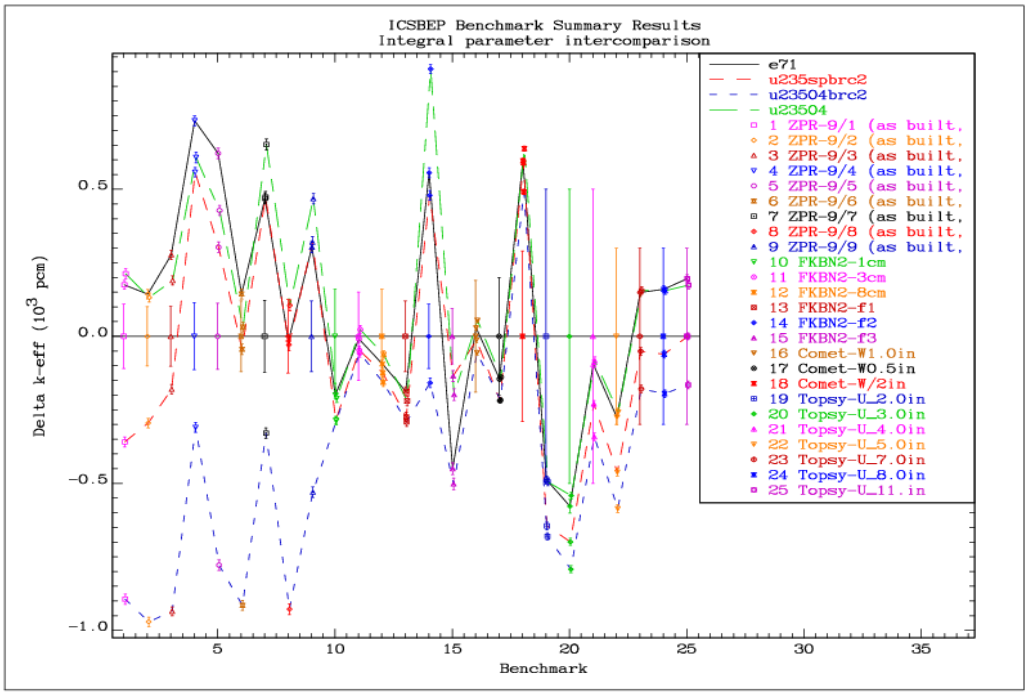

Figure 22: Results for tungsten benchmarks.

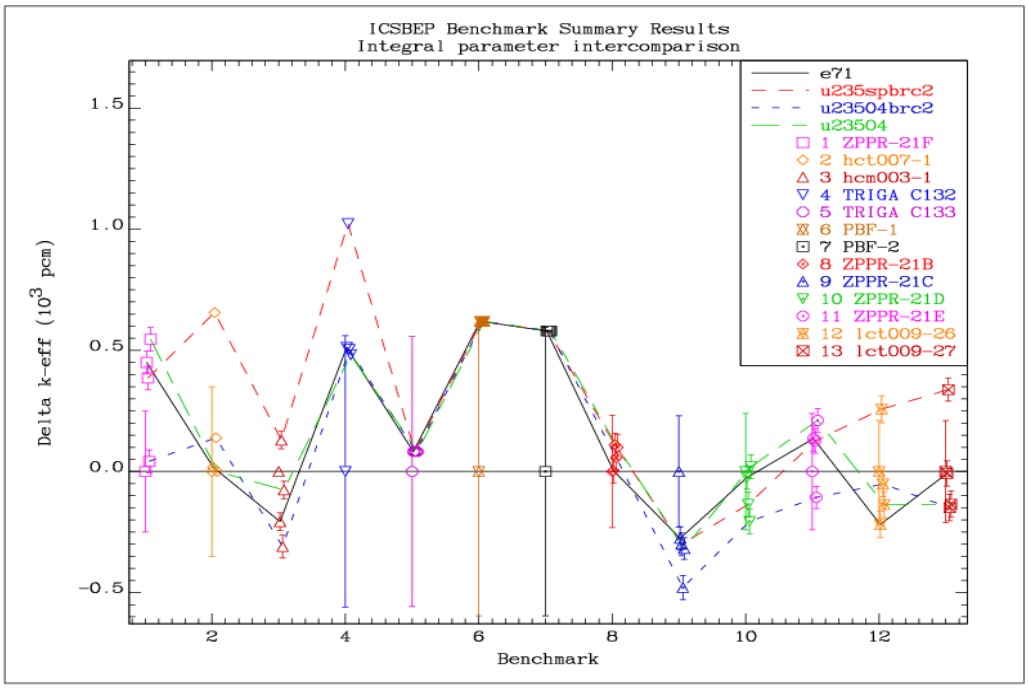

Figure 23: Results for zirconium benchmarks.

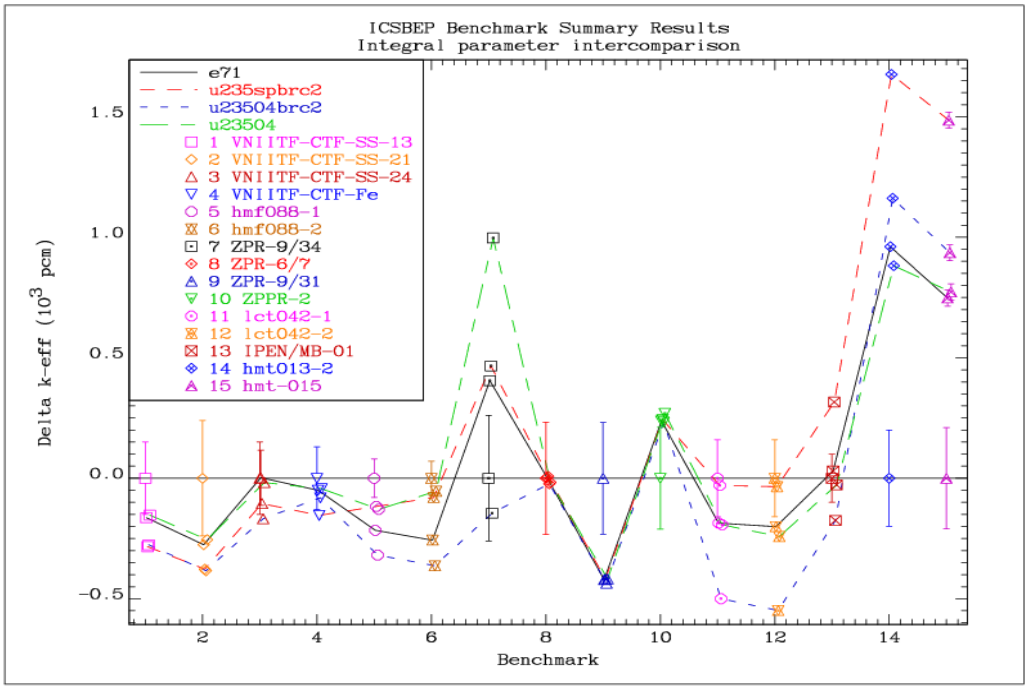

Figure 24: Results for iron benchmarks.